ISSN 0030-400X, Optics and Spectroscopy, 2015, Vol. 118, No. 2, pp. 277–283. © Pleiades Publishing, Ltd., 2015.
Original Russian Text © V.A. Shvets, V.N. Kruchinin, S.V. Rykhlitskii, V.Yu. Prokop'ev, N.F. Uvarov, 2015, published in Optika i Spektroskopiya, 2015, Vol. 118, No. 2, pp. 292–299.

CONDENSED-MATTER SPECTROSCOPY

Ellipsometric in situ Diagnostics of the Growth of Porous Anodic Oxide Films on Aluminum

V. A. Shvets[a, b], V. N. Kruchinin[a], S. V. Rykhlitskii[a], V. Yu. Prokop'ev[a, b], and N. F. Uvarov[c]

[a] *Rzhanov Institute of Semiconductor Physics, Siberian Branch, Russian Academy of Sciences, Novosibirsk, 630090 Russia*

[b] *Novosibirsk State University, Novosibirsk, Russia*

[c] *Institute of Solid-State Chemistry and Mechanochemistry, Siberian Branch, Russian Academy of Sciences, Novosibirsk, 630128 Russia*

e-mail: shvets@isp.nsc.ru

Received September 12, 2013; in final form, July 7, 2014

Abstract—An ellipsometric in situ study of the growth of porous aluminum anodic oxide films on aluminum substrate has been performed. Theoretical calculations have been carried out to interpret the experimental dependences of ellipsometric parameters; they made it possible to identify the most characteristic details of anodic oxidation. It is shown that the ellipsometric method allows one to control in situ in real time a number of important layer parameters: growth rate, porosity, depth uniformity, and the state of interface. The ellipsometric measurements have also revealed high sensitivity to the presence of metal nanoparticles both in the bulk of a layer and on its surface.

DOI: 10.1134/S0030400X15020162

INTRODUCTION

Much attention has been paid to mesoporous films in the last two decades [1, 2]. The reason for this is that these films, being grown under certain conditions, exhibit high porosity and a small spread of pore diameters. Hence, they are considered as promising materials for inorganic membranes, filters, calibration grids with a nanoscale period [3], carriers for heterogeneous catalysts, and functional nanocomposites and nanoreactors [4–6].

Anodic oxide Al_2O_3 is an X-ray amorphous solid material, composed of hydrated aluminum oxide $Al_2O_3^{\bullet}(H_2O)_n$, where $n = 0–3$ [3, 5]. The microstructure of an anodic aluminum oxide film formed on the surface of aluminum is determined by several factors. The most important ones are the electrolyte type, anodic oxidation potential, and temperature.

It is known that anodic oxidation of aluminum in aqueous solutions of acids (such as oxalic, phosphoric, sulfuric, or chromic) at a certain concentration leads to the formation of a porous structure [7], in which the diameter of pores and distance between them can be varied by changing anodic oxidation potential. These films consist of an internal thin layer (referred to as a barrier) and an external porous layer. The thickness of the former is varied by changing the anodic oxidation potential; it generally amounts to several tens of nanometers. The thickness of the former layer is determined by the anodic oxidation time and the film growth rate, which depends strongly on the electrochemical cell potential and the electrolyte composition and temperature [8].

Thus, the processes of growth and characteristics of anodic oxide films exhibit high variability and depend on a number of technological parameters. There are only a few methods compatible with anodic oxidation, which would make it possible to observe in situ the growth kinetics and monitor the properties of grown films. One of these methods is ellipsometry, which is sensitive to the density and thickness of growing layers and allows one to characterize the structural properties of material, quality of interface, etc. However, ellipsometry is not a direct method; therefore, to characterize the aforementioned parameters, one must perform preliminary simulation of the growth processes in order to develop the corresponding diagnostic technique.

In this paper, we report the results of analyzing the in situ ellipsometric data obtained during growth of oxide films on aluminum and report developed techniques for their interpretation.

EXPERIMENTAL

Ellipsometry

Ellipsometric measurements are based on the change in the polarization state of a light wave reflected from a surface. The experimentally measured

ellipsometric parameters Ψ and Δ describe the changes in the wave amplitude and phase. These parameters are related to the complex reflection coefficients for waves polarized in the plane of incidence (R_p) and in the perpendicular direction (R_s) by the expression

$$\tan\Psi e^{i\Delta} = \frac{R_p}{R_s}. \quad (1)$$

Reflection coefficients R_p and R_s depend on environment refractive index n_0, the optical constants of the layers in the structure under study, their thicknesses, and the angle of incidence of light φ and light wavelength λ. A single-layer "substrate–layer" system is described by the formulas [9]

$$R_{p,s} = \frac{(r_{01p,s} + r_{12p,s}X)}{(1 + r_{01p,s}r_{12p,s}X)}, \quad (2)$$

where r_{01} and r_{12} are the Fresnel coefficients for the "environment–film" and "film–substrate" interfaces, respectively;

$$X = -4\pi i(d/\lambda)\sqrt{N_1^2 - \sin^2\varphi}$$

is the exponential function of phase thickness; $N_1 = n_1 - ik_1$ is the complex refractive index of the film; and d is its thickness. In the case of a two-, three-, or n-layer system, reflection coefficients $R_{p,s}$ are calculated applying recurrence relations, the structure of which is similar to that of Eq. (2). Using the expressions for the reflection coefficients and Eq. (1), one can analytically relate the measured values Ψ and Δ with the parameters of the structure under study. The optical constants of layers are generally set using reference data. Effective refractive index N_{eff} of composition (heterogeneous) media is calculated from the Bruggeman relation [10]:

$$\sum_i q_i \frac{N_i^2 - N_{\text{eff}}^2}{N_i^2 + 2N_{\text{eff}}^2} = 0, \quad (3)$$

where N_i are the complex refractive indices for each component and q_i is the volume fraction of this component; $\sum q_i = 1$. Using relation (3), one can calculate the refractive index of a porous layer, considering it as a mixture of the matrix material with air ($N_{\text{air}} = 1$) or electrolyte ($N_{\text{el}} = 1.332$).

Experimental Technique

The initial samples were 0.5-mm-thick plates of technical-purity aluminum of grade A5 (*GOST* (State Standard) 11069-2001). To obtain the surface state applicable for ellipsometric measurements, the samples were mechanically polished to high luster by diamond pastes and washed in distilled water. Check measurements of the initial substrates were performed ex situ on the spectral ellipsometer described in [11] (in the wavelength range of 250–1100 nm). Its spectral resolution was 2 nm; the angle of incidence of the light beam on the sample was 70°.

To study in situ the anodic oxidation processes, we designed a setup containing an electrochemical cell matched with a high-speed laser ellipsometer [11]. The anode was an aluminum sample, and the cathode was a stainless steel grid. An aqueous solution of 0.3 M oxalic acid was used as an electrolyte. Anodic oxidation was performed in the dc mode; the dc voltage was varied from experiment to experiment in the range of 30–100 V. The cell had fused silica windows for input and output of probe radiation; the residual birefringence in these windows was minimized. The angle of incidence of a laser beam on a sample was 64.55°. Measurements were performed with an interval of 0.1 s. The anodic oxidation time in different experiments varied from 1.5 min to 2 h. Electrolyte was removed from grown films by washing them in distilled water; the films were then dried in air and additional measurements on a spectral ellipsometer were carried out (see above).

RESULTS

Data of spectral ellipsometric ex situ measurements were used to calculate (using the model of a semi-infinite medium [12]) the spectra of optical constants of Al substrates. Comparison of the obtained results with the data in the literature for aluminum [13, 14] shows that the measured and reference spectra of optical constants behave similarly but differ quantitatively. These differences may be due to both the properties of the technical aluminum used and to the specific features of surface preparation. The reproducibility of ellipsometric measurements from substrate to substrate was $\pm 1.5°$ and $\pm 2°$ for Ψ and Δ, respectively. The average values of the refractive and absorption indices for wavelength $\lambda = 632.8$ nm were $n_{\text{Al}} = 2.4$ and $k_{\text{Al}} = 5.0$. Furthermore, when interpreting ellipsometric data, the n and k values corresponding to a specific substrate were chosen in each calculation. This approach allowed us to take into account the individual features of optical properties of a given substrate and use most efficiently ellipsometry as a differential analytical method.

Figure 1 shows characteristic experimental dependences of the ellipsometric parameters (Δ–Ψ), measured during growth of anodic oxide films (growth curves). These results were obtained by varying the anode voltage and electrolyte temperature. It can be seen that experimental trajectories have a cyclic or quasi-cyclic character and highly diverse shapes. The initial growth stage is characterized by rather fast (1–3 s) changes in Ψ and Δ (the *AB* segment in Fig. 1a), which are related to the formation of a barrier layer with somewhat different optical properties. The next stages

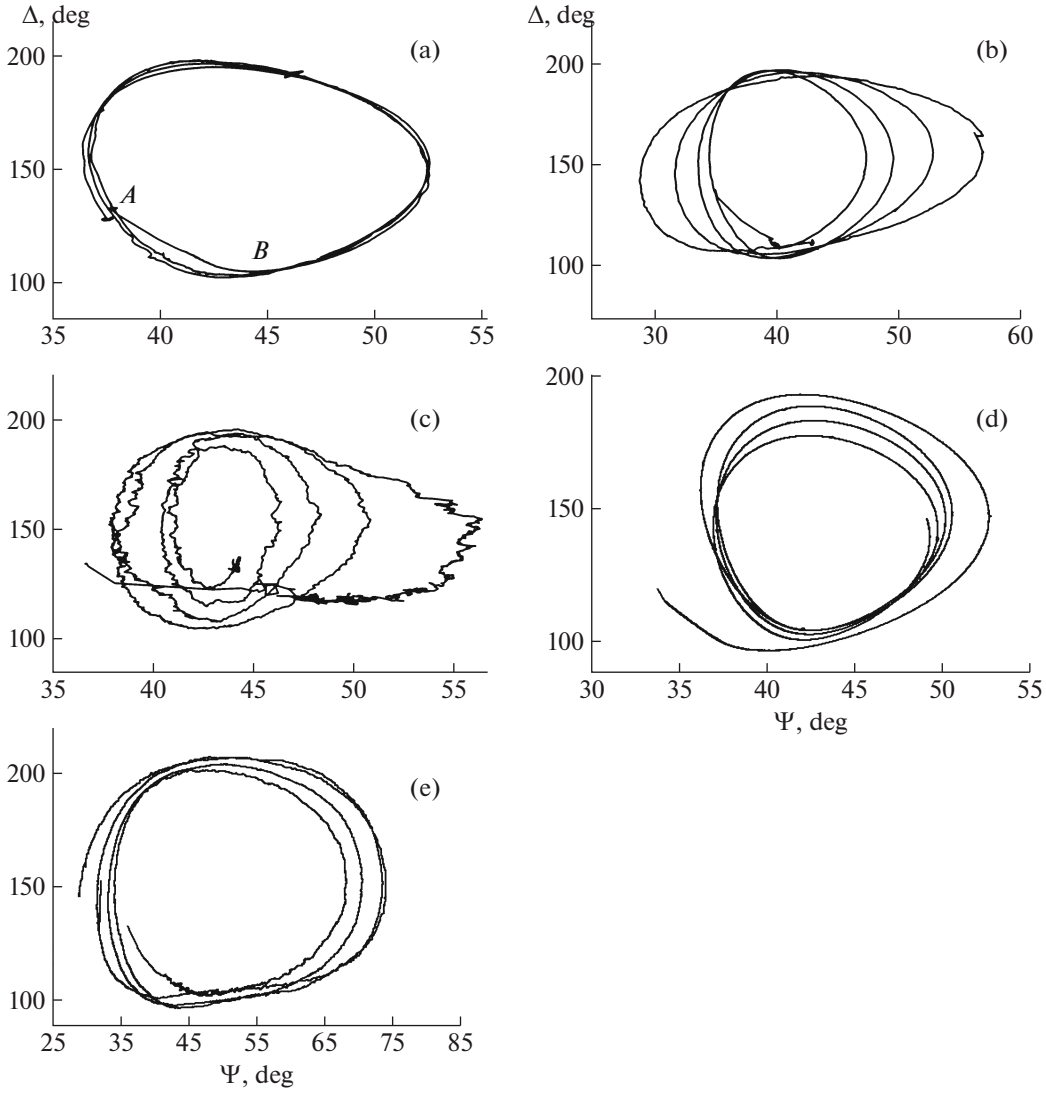

Fig. 1. Experimental growth curves for Al_2O_3 films on an aluminum substrate, obtained at anode voltages of (a) 30, (b) 40, (c) 60, (d) 50, and (e) 40 V and electrolyte temperatures of (a) 24 and (b–e) 4°C.

of film formation are accompanied by slower changes in the ellipsometric parameters.

According to formula (2), in the case of growth of a homogeneous transparent layer, the ellipsometric parameters should change cyclically along the same trajectory with the interference period. Indeed, this experimental dependence is observed in Fig. 1a. At the same time, some experiments yielded trajectories in which the peak-to-peak turn increases with the number of cycle (Fig. 1b) or, vice versa, decreases (Fig. 1c). In some experiments we observed rolling-up turns shifted down along the Δ axis (Fig. 1d). Trajectories with an anomalously large deviation of parameter Ψ were also observed (Fig. 1e). To explain this variety, we modeled the growth curves and considered the main factors affecting the ellipsometric data.

MODELING OF GROWTH CURVES

According to Eq. (2), an increase in the thickness of dielectric nonabsorbing layer should be accompanied by a cyclic change in the ellipsometric parameters with the interference period

$$d_0 = \lambda/2\sqrt{n_1 - \sin^2\varphi},$$

where n_1 is the refractive index of the layer. The n_1 value for a porous film is calculated from Bruggeman relation (3); depending on the total porosity ($p = V_{f.}/V_{sum}$, where $V_{f.}$ and V_{sum} are, respectively, the specific volumes of pores and the entire film), n_1 may change from 1 (refractive index of air) to 1.76 (refractive index of Al_2O_3 at $\lambda = 632.8$ nm [15]). Figure 2 shows a nomogram: a set of calculated growth trajectories corresponding to different values of material porosity, which is determined as the volume fraction

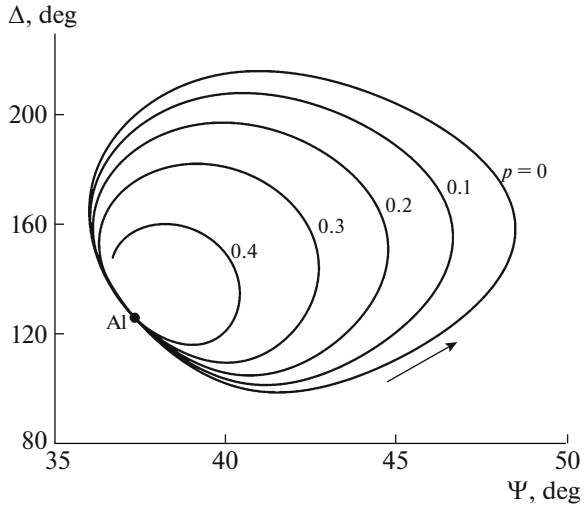

Fig. 2. Calculated growth nomograms for porous Al_2O_3 films on an aluminum substrate at different values of total film porosity. The arrow indicates the direction of variation in the ellipsometric parameters during film growth. The point in the Ψ–Δ plane corresponds to the aluminum substrate.

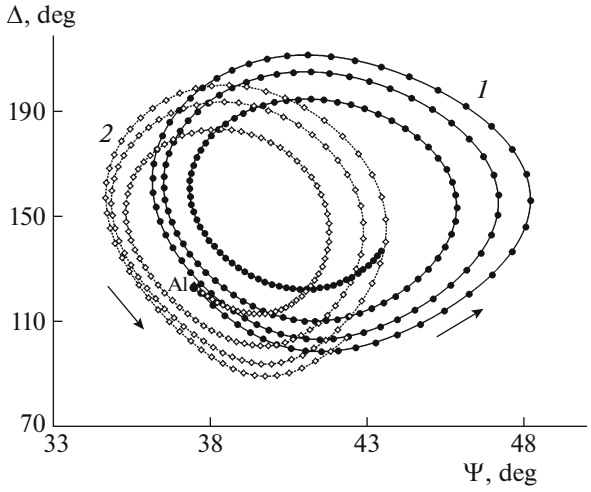

Fig. 3. Calculated growth curves for a layer with a porosity linearly varying over depth. Curves *1* (circles) correspond to a change in porosity from $p = 0$ near the substrate to $p = 0.4$ on the surface, and curves *2* (diamonds) correspond to the change in porosity from $p = 0.4$ near the substrate to $p = 0$ on the surface. The layer thickness for each curve is 1000 nm. The point corresponding to the substrate is indicated as Al, and the arrow indicates the direction of plotting curves during film growth.

of pores and assumed to be constant along the layer depth.

It can be seen that the peak-to-peak amplitude of the curves decreases with an increase in porosity and degenerates into a point near $p = 0.45$. This occurs for the following reason: with an increase in p, the refractive index of a porous film approaches the refractive index of the environment (for an aqueous electrolyte solution, $n_0 = 1.332$), which, in turn, reduces the optical contrast between the layer and medium. Based on this nomogram, one can conclude that growth curves are sensitive to porosity and, hence, can be used to determine experimentally this important parameter. In addition, the kinetics of change in the ellipsometric parameters allows one to calculate easily the growth rate of anodic film and its final thickness if the curves are calibrated to thickness. For example, the experiment in Fig. 1a revealed three interference cycles, and the film thickness turned out to be 933 nm. A comparison of the experimental growth curve in Fig. 1a with the calculation nomogram suggests also that the above-mentioned barrier layer has a lower density, because the corresponding portion of the curve lies within the cyclic trajectory.

Using the nomogram presented in Fig. 2, one can explain the experimentally observed growth curves with unrolling (Fig. 1b) and rolling up (Fig. 1c) turns. If porosity increases monotonically with an increase in the film thickness, the corresponding curve should pass from external turns of the nomogram to internal ones, i.e., roll up. If the porosity decreases, the situation is reversed and one has an unrolling cyclic curve. This is confirmed by calculations the results of which are presented in Fig. 3 for a linear monotonic change in the growing film porosity from 0 to 0.4.

Indeed, curves with unrolling or rolling up turns (depending on the sign of change in porosity) are observed in this case. A comparison of these curves with the nomogram in Fig. 2 shows that the current values of ellipsometric parameters for a film with changing porosity do not determine the porosity value at a given point. If we consider the ellipsometric parameters and porosity as functions of thickness z, the relationship between $\Psi(z)$ and $\Delta(z)$, on the one hand, and $p(z)$, on the other hand, is not local but integral. Therefore, the current Ψ and Δ values depend on the history of change in $p(z)$. Nevertheless, the current porosity value can be estimated from the amplitude of the last interference turn; the best candidate for this estimation is the amplitude of change in parameter Δ.

The curves in Fig. 3 explain one of the possible reasons for the violation of growth curve cyclicity. Nevertheless, the discrepancy between turns in the calculated curves is not so large, despite the significant change in porosity, which was taken into account in the calculations. This result is inconsistent with some experimental curves, which exhibited a much more pronounced increase in the cycle amplitude.

Another cause of cyclicity violation may be related to the absorption of light in the film. Optical absorption in the growing film may be due to the presence of metallic inclusions. Estimates based on the Bruggeman relation show that the presence of 1 vol % Al

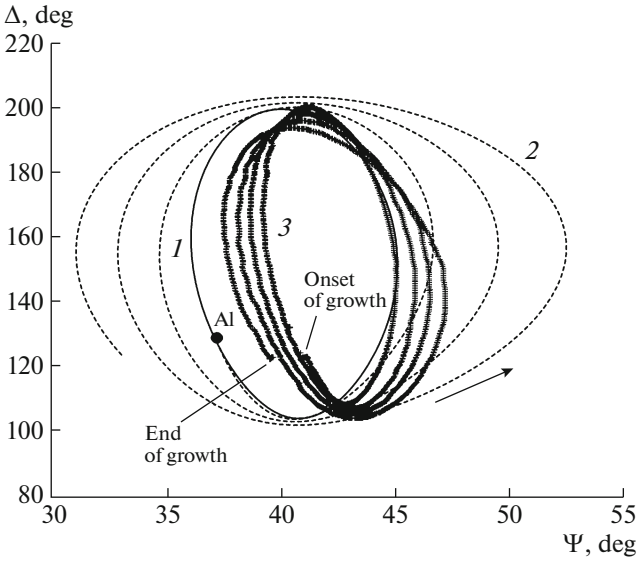

Fig. 4. Growth curves for a nonabsorbing porous Al_2O_3 film (*1*, solid line) and a film with absorption index $k = 0.01$ (*2*, dashed lines). The calculation was performed for a 1000-nm film with porosity $p = 0.2$. The designations are the same as in Fig. 3. Curve *3* (crosses) is an experimental growth curve with unrolling turns.

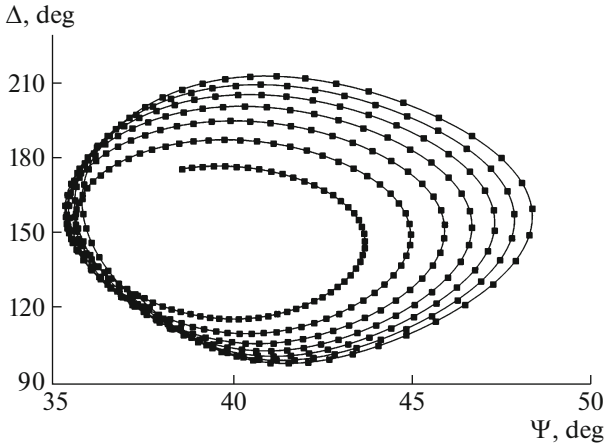

Fig. 5. Calculated trajectory modeling the development of relief at the film–substrate interface. During growth of a film, its parameters change proportionally to the film thickness: the porosity changes from 0 to 0.4, and the relief height grows from 0 to 10 nm. The final film thickness is 2 μm.

inclusions leads to absorption characterized by $k \sim 0.01$. The growth curve calculated with allowance for this absorption is shown in Fig. 4 (curve *2*). For comparison, a calculated trajectory for a nonabsorbing film (curve *1*) and one experimental dependence (curve *3*) are also shown. As follows from the calculation, absorption leads to unrolling of turns during film growth and increase in the amplitude of variation in ellipsometric parameters. The distance between the turns of calculated spiral is proportional to the absorption magnitude. Varying absorption, one can obtain qualitative correspondence between the calculated and experimental curves. For example, having compared the pitch for the calculated and experimental trajectories presented in Fig. 4, we find the absorption value for the experimental trajectory to be $k = 0.003$.

Better fitting results can be obtained by optimizing two parameters: porosity gradient and absorption. However, growth curves with turns embedded into each other without self-crossings are observed in both cases. At the same time, some experiments demonstrated a monotonic displacement of turns, preferably downward along the Δ axis. This displacement is generally accompanied by a decrease in their amplitude (Fig. 1d). As was noted above, a decrease in the turn amplitude is indicative of increase in porosity in the direction towards the surface (Fig. 3, curve *1*).

The displacement of turns is unambiguously related to the change in optical properties of the Al substrate–film interface. Indeed, in the case of a homogeneous film with zero absorption, the growth curve should pass through the initial point (corresponding to the substrate) each time when the interference period is over (this point is marked as "Al" in Fig. 2). If the interface changes during growth (an example is the development of a microrelief), the initial point is shifted, leading to displacement of turns of the ellipsometric dependence Δ–Ψ. Figure 5 shows a calculated curve for the case in which the film growth is accompanied by a simultaneous change in porosity from 0 to 0.4 and development of relief at the interface, the sizes of which increase from 0 to 10 nm. Indeed, the calculated growth curve is similar to the experimental curve in Fig. 1d, although its turns are shifted along both the Δ and Ψ axes. This fact indicates that the processes occurring at the interface are more complicated and are not reducible to only morphological changes. Therefore, the experimentally observed displacement of turns should be considered as an indicator of instability of the optical properties of the interface.

In some experiments, we observed an anomalously large amplitude of variation in parameter Ψ. Figure 1e shows a curve where parameter Ψ reaches 75°. None of the above-considered factors (variation in porosity, absorption in the layer, and development of transition layer) can explain this behavior of growth curves. Among these factors, the absorption in the film affects most strongly the amplitude of variation in Ψ. However, it can be clearly seen in Fig. 4 that this effect results in the displacement of both right and left boundaries of the growth curves with respect to the substrate point, which contradicts the experimental results.

For one of the samples, the growth of which was characterized by a large amplitude of variation in Ψ, we measured ex situ spectra of ellipsometric parame-

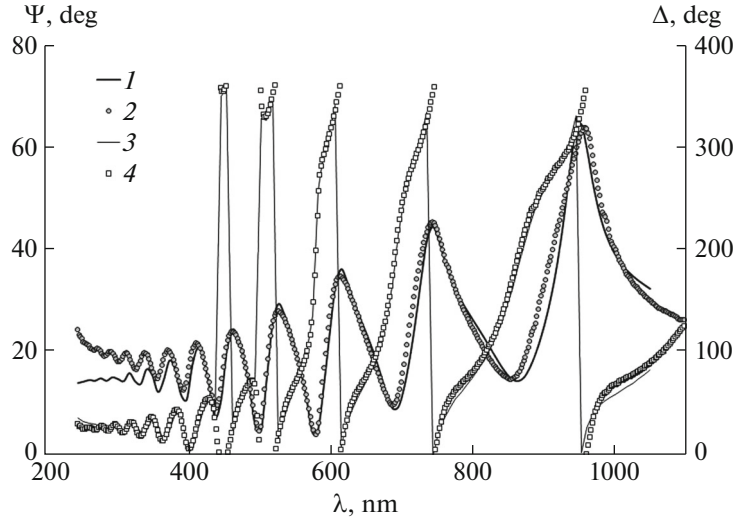

Fig. 6. Experimental (*2*, *4*) and calculated (*1, 3*) spectral dependences of ellipsometric parameters (*1*, *2*) Ψ and (*3, 4*) Δ for a sample with an anodic oxide film on Al.

ters (Fig. 6). The experimental spectra can be described within the "substrate–transition Al layer + oxide (54 nm)–oxide layer (1236 nm)–Al layer (1.3 nm)" three-layer model. The calculated spectra corresponding to this model are also shown in Fig. 6; they are in fairly good agreement with the experiment. It is of fundamental importance that this agreement between experimental and theoretical spectra can be obtained only when the transition and surface layers are taken into consideration. The transition layer is what one would expect: it is a mixture of aluminum and oxide, which can be interpreted as the interface microrelief. At the same time, the presence of a thin surface Al layer is unexpected. Nevertheless, exclusion of this layer from the model leads to disagreement between the experimental and calculation results. The presence of metallic aluminum on the surface of anodic film is also confirmed by X-ray photoelectron spectroscopy data, which were obtained several days after the film growth. The fact that aluminum has not enough time to become oxidized after this period indicates that we deal with rather large metallic clusters, which may be several tens or several hundreds of nanometers in size. We believe that these clusters can be formed during polishing substrates and remain in some amounts after incomplete washing. During growth these nanoparticles are partially distributed over the film bulk in the form of inclusions (and become responsible for absorption in it) and partially move jointly with the interface, thus remaining on the surface. Proceeding from the above-determined effective thickness of this "layer" of metal particles, one can determine their surface density at a level of 10^6–10^8 cm^{-2}.

With allowance for the results obtained, we calculated the growth curves for an anodic film with aluminum particles on the surface, which were modeled by a thin layer of constant thickness (Fig. 7). It was found that the presence of this layer (with a thickness as small as 2 nm) leads to a significant displacement of the right boundary of the growth curve to larger Ψ values; this displacement is comparable with the experimentally observed one. At the same time, the left boundary is not displaced and the curve passes through the initial growth point in each cycle. This behavior can easily be explained: at thicknesses of the oxide film multiple of the interference period, its contribution to reflection

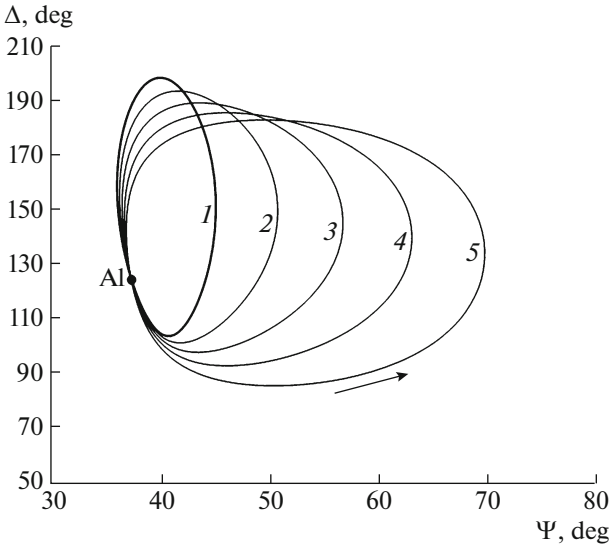

Fig. 7. Growth curves calculated according to the "Al substrate–porous film–Al surface layer" model for a total porosity $p = 0.2$. The thickness of the Al surface layer is (*1*) 0, (*2*) 0.5, (*3*) 1, (*4*) 1.5, and (*5*) 2 nm.

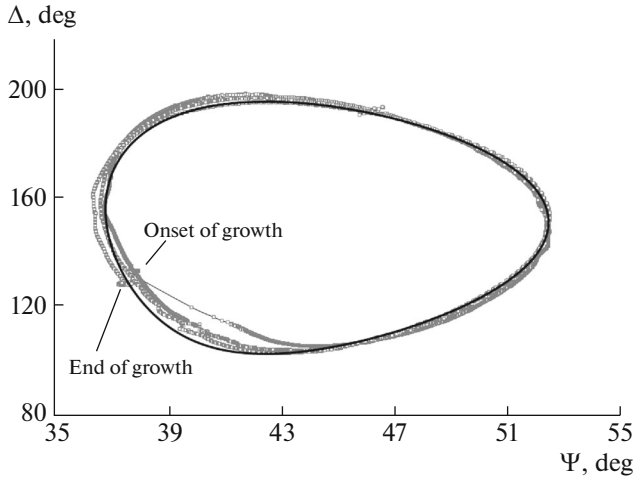

Fig. 8. Comparison of experimental (squares) and theoretical (solid line) growth curves. The model parameters for calculating the theoretical curve are given in the text.

disappears and the "Al substrate–anodic film–Al layer" system becomes equivalent to the "Al substrate–Al film" system; i.e., the properties of the reflected light are the same as in the case of pure reflection from the substrate. Comparison of the modeling results with the experimental data shows that the growth of anodic oxide on aluminum is accompanied by different processes, which must be taken into account to interpret ellipsometric data quantitatively. Such an interpretation was performed for the experimental data presented in Fig. 1a. As a result, we developed a model most adequately describing the experimental growth curve. This model includes a transition layer ($n = 1.65$, $k = 0.015$, $d =$ 400 nm), the main porous oxide layer with refractive index $n = 1.6$ (corresponding to porosity $p = 0.1$), and a surface aluminum layer with an effective thickness of 0.4 nm. Taking into account the slight divergence of experimental-curve turns, one can obtain the above determination for absorption in a growing film: $k <$ 0.0005, a value that corresponds to the volume content of aluminum inclusions at a level of ~0.05%. It is noteworthy that the turn for the initial growth stage corresponding to the formation of a barrier layer somewhat differs from the subsequent turns and from the calculated curve. This means that changes occurred near the interface during growth, which led to the effect observed (Fig. 8).

CONCLUSIONS

We performed an in situ ellipsometric study of the growth of porous anodic oxide layers on an aluminum substrate. The observed experimental regularities were explained taking into consideration the main factors that may affect the results of ellipsometric experiment: film porosity, optical absorption in the film bulk, processes on the interface, and the presence of metal clusters on the surface. Our modeling showed that the aforementioned factors can explain the experimentally observed variety of growth curves. Hence, real-time ellipsometry can be used for in situ monitoring of the processes of anodic film growth. In particular, one can monitor such characteristics as the quality of preparation of the initial substrates, porosity of anodic layers and their growth rate, and the presence of aluminum nanoparticles in the film bulk and on the film surface.

REFERENCES

1. R. C. Furneaux, W. R. Rigby, and A. P. Davidson, Nature **337**, 147 (1989).
2. G. E. J. Poinern, A. Nurshahidah, and D. Fawcett, Materials **4**, 487 (2011).
3. K. S. Napol'skii, I. V. Roslyakov, A. A. Eliseev, A. V. Lukashin, V. A. Lebedev, D. M. Itkis, and Yu. D. Tret'yakov, Al'tern. Energ. Ekol., No. 11, 79 (2009).
4. A. P. Karnaukhov, *Adsorption. Texture of Dispersed and Porous Materials* (Nauka, Novosibirsk, 1999) [in Russian].
5. S. Pillet, M. Souhassou, C. Lecomte, K. Schwarz, P. Blaha, M. Rérat, A. Lichanot, and P. Roversi, Acta Crystallogr. A **57**, 290 (2001).
6. M. J. Pellin, P. C. Stair, G. Xiong, J. W. Elam, J. Birrel, L. Curtiss, S. M. Georg, C. Y. Han, L. Iton, H. Kung, M. Kung, and H.-H. Wang, Catalysis Lett. **102** (3–4), 127 (2005).
7. G. D. Sulka, *Highly Ordered Anodic Porous Alumina Formation by Self-Organized Anodizing. Nanostructured Materials in Electrochemistry,* Ed. by A. Eftekhari (WILEY-VCH, Weinheim, 2008), p. 1.
8. J. W. Diggle, T. C. Downie, and C. W. Goulding, Chem. Rev. **69**, 365 (1969).
9. A. V. Rzhanov, K. K. Svitashev, L. V. Semenenko, and V. K. Sokolov, *Principles of Ellipsometry* (Nauka, Novosibirsk, 1978) [in Russian].
10. D. E. Aspnes, Thin Solid Films **89**, 249 (1982).
11. E. V. Spesivtsev, S. V. Rykhlitskii, and V. A. Shvets, Avtometriya **47** (5), 5 (2011).
12. R. M. Azzam and N. M. Bashara, *Ellipsometry and Polarized Light* (North-Holland, Amsterdam, 1977; Mir, Moscow, 1981).
13. E. Palik, *Handbook of Optical Constants of Solids* (Academic, New York, 1985).
14. *Thematic Databases of the Physico-Technical Institute im. A.F. Ioffe: New Semiconductor Materials*; n k database, http://www.ioffe.ru/SVA/NSM/nk/index.html.
15. V. M. Zolotarev, V. N. Morozov, and E. V. Smirnova, *Optical Constants of Natural and Technical Media: A Handbook* (Khimiya, Leningrad, 1984) [in Russian].

Translated by Yu. Sin'kov